Available online at www.sciencedirect.com

SciVerse ScienceDirect

Ceramics International 39 (2013) 1075–1079

CERAMICS INTERNATIONAL

www.elsevier.com/locate/ceramint

Effects of solid content on the phase assemblages, mechanical and dielectric properties of porous α-SiAlON ceramics fabricated by freeze casting

Zhaoping Hou*, Feng Ye, Limeng Liu, Qiang Liu, Haijiao Zhang

School of Materials Science and Engineering, Harbin Institute of Technology, Harbin 150001, China

Received 24 June 2012; accepted 6 July 2012
Available online 20 July 2012

Abstract

Porous Y-α-SiAlON ceramics were prepared by freezing camphene-based suspensions at 0 °C and subsequently sintering at 1900 °C for 1 h. The effects of solid loading content in the suspensions on porosities and formation of α-SiAlON as well as mechanical and dielectric properties of the porous ceramics were investigated. An XRD analysis performed on sintered samples indicated that the α-SiAlON did not fully form in the sample with initial solid loading content of 10 vol%, due to the high porosity of 90 vol% and interconnected pore of the green body. With the increase of initial solid loading content from 10 vol% to 30 vol%, the porosity decreased from 62.3% to 23.1% and the average pore size decreased from 19 μm to 8 μm. As a result, the flexural strength increased significantly from 72.4 MPa to 190.2 MPa, fracture toughness increased from 1.20 MPa m$^{1/2}$ to 3.48 MPa m$^{1/2}$, as well as the dielectric constant increased from 3.3 to 6.3. The dielectric loss (tan δ) of obtained material varied between 1.4×10^{-2} and 2.8×10^{-2}, which did not depend on the porosity of samples.

Keywords: C. Mechanical properties; Porous α-SiAlON; Freeze casting; Dielectric constant

1. Introduction

Porous ceramics containing tailored porosity exhibit special properties and features that usually cannot be achieved by the conventional dense counterparts. The advantages of porous ceramics are the combination of these inherent properties of ceramics and the features obtained by drawing voids into the component. Such features include low density, low thermal conductivity, high surface area, controlled permeability, high specific strength and low dielectric constant. Therefore, porous ceramics with high porosity have attracted much attention for industrial applications, especially for environments where high temperatures and corrosive media are involved, such as hot gas filters, catalyst supports, particle filters and gas membranes [1]. For these applications, it is important to tailor these properties of porous material by controlling the porosity and pore structure, such as open or closed pore, pore morphology and pore size distribution.

Recently, the freeze casting has attracted an increasing interest, since it can produce well-defined pore structures replicating the shapes of the connected frozen solvent crystals [2]. A wide variety of ceramic materials have already been tested by freeze casting, including Al_2O_3, Si_3N_4, SiC and ZrO_2 [3–6]. With regard to oxide-based ceramics, such as Al_2O_3 and ZrO_2, they have superior oxidation and corrosion resistance but poor strength and poor thermal shock resistance. Compared to oxide-based ceramics, Si_3N_4 ceramics exhibit good thermal shock resistance [7], while they did not demonstrate good corrosion resistance because of the sintering additives which are necessary to densification and phase transformation of Si_3N_4. SiAlON ceramics that are solid solutions of Si_3N_4 offer the advantages of incorporating some sintering additives into the Si_3N_4 lattice and hence reducing the amount of glassy phase, consequently improving corrosion resistance [8]. Therefore, SiAlON ceramics should be

---

*Corresponding author. Tel./fax: +86 451 86413921.
E-mail address: houzhaoping@yahoo.cn (Z. Hou).

0272-8842/$ - see front matter © 2012 Elsevier Ltd and Techna Group S.r.l. All rights reserved.
http://dx.doi.org/10.1016/j.ceramint.2012.07.029

good candidates for porous ceramics in high temperature applications.

To date, the freeze casting has not been used for fabricating porous SiAlON ceramics. SiAlON ceramics are commonly produced by reaction sintering of α- or β-Si_3N_4, Al_2O_3, AlN and R_2O_3. In the case of aqueous freeze casting, AlN powder will be hydrolyzed by water when in contract with water [9]. In order to limit AlN hydrolysis, camphene was a good candidate as organic solvents in the preparation of SiAlON slurry. In addition, as camphene has a melting temperature of 44–48 °C [10], the freeze casting process can be carried out at near room temperature and the frozen camphene can be removed via sublimation without any assistance of device, thus allowing more flexible processing.

For these reasons, the camphene based freeze casting method was used to fabricate porous α-SiAlON ceramics in this work. The sintered porous α-SiAlON ceramics were thoroughly characterized in order to establish the effect of initial solid loading on the phase assemblage and pore microstructure characteristics as well as mechanical and dielectric properties of the final product.

2. Experimental procedure

According to the general chemical formula $Y_{m/3}Si_{12-(m+n)}Al_{(m+n)}O_nN_{16-n}$, the composition of α-SiAlON corresponding to $m=1.0$, $n=1.0$ was investigated in our experiments. Starting powders used to prepare the porous SiAlON ceramics are α-Si_3N_4 (SN-E10, containing 1.27% oxygen, UBE Industries, Japan), Al_2O_3 ($>99.9\%$, 0.5 μm, A16-SG, Alcoa, USA), AlN (grade C, H.C. Stark, Berlin, Germany), and Y_2O_3 ($>99.9\%$, grade fine, H.C. Stark, Berlin, Germany). When calculating the overall compositions, 2.38 wt% SiO_2 and 1.83 wt% Al_2O_3 on the surface of Si_3N_4 and AlN powders were taken into account respectively.

Different solid loading content (10 vol%, 20 vol%, 30 vol%) slurries containing the SiAlON precursor were prepared using HAO FAST 923 (Shanghai Haoyang Co., Ltd., Shanghai, China) as a dispersant in camphene (95% Purity, Guangzhou Huanpu chemical Factory, Guangzhou, China), following by ball milling at 60 °C for 24 h in sealed bottles. All of the prepared slurries exhibit excellent flowability for casting, regardless of the initial solid loading.

Immediately after the resultant warm slurries were poured into polyethylene molds (Ø 60 mm × 10 mm) which were pre-warmed at 60 °C, the molds and slurries were set on a copper plate immersed in ice-water mixture at 0 °C for freezing.

Thereafter, the green bodies were placed on a polyurethane sponge in open air at room temperature for about 4 days to sublime the solidified camphene in the green compacts. Sintering was performed in a conventional graphite resistant furnace at 1900 °C for 1 h under a nitrogen-gas pressure of 0.6 MPa. A BN-Si_3N_4 powder bed (50 wt% BN, 50% Si_3N_4) was used. The heating and cooling rates were both 10 °C/min.

The porosities and pore size distribution were measured by mercury porosimetry (Autopore 9500, Micrometics Co., UAS). Crystalline phases of the produced porous ceramics were characterized by X-ray diffraction (XRD). The microstructures of the sintered samples were observed from the fractures samples using a scanning electron microscope (SEM).

Flexural strength and fracture toughness were measured by three-point flexure and single-edge-notched beam (SENB) tests respectively. Each date point marks an average of six measurements.

The dielectric properties of obtained porous Y-SiAlON ceramics were measured by the method of waveguide using a vector network analyzer (Agilent E8362B) over 12.4–18 GHz. The sizes of measured samples were 7.9 mm × 15.8 mm × 2.0 mm.

3. Results and discussion

3.1. Phase formation

Fig. 1 shows the XRD patterns of obtained porous α-SiAlON ceramics with different initial solid loading content sintered at 1900 °C for 1 h. There were two phases α and β-SiAlON detected in the samples with initial solid loading content of 10 vol%. No secondary crystalline phases were detected by XRD, which shows that the cooling rate is sufficient to prevent crystallization of gain boundary glass. When the initial solid loading content increased to 20 vol%, the intensity of peak of β-SiAlON was decreased significantly. With further increase to 30 vol%, only α-SiAlON was detected without any amount of detectable second phase. Thanks to the unique freezing process, the green bodies have a highly packed ceramic powder network with high green density $>50\%$ [11],

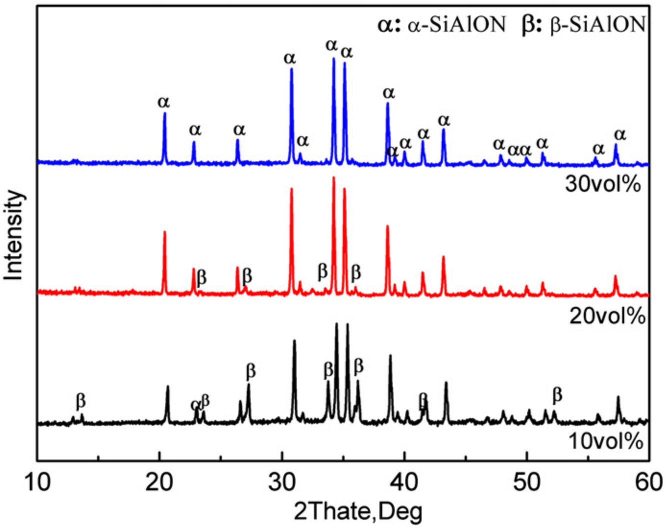

Fig. 1. XRD patterns of porous α-SiAlON ceramics with different solid loading contents sintered at 1900 °C for 1 h.

regardless of the initial solid loading content, which accordingly makes it possible to enable the mixed powders to react completely and mostly form SiAlON phases. However, for the green body of 10 vol% solid loading content with higher porosity (90%) and open pores, for evaporation of chemicals on the surface of ceramic walls is inevitable , resulting in incomplete formation of α-SiAlON [12].

3.2. Porosities and pore structures

The porosities and pore size distributions of fabricated samples were characterized by mercury porosimety and are summarized in Table 1. The porosity of obtained porous Y-SiAlON ceramics decreased proportionately from 64.3% to 23.1% with the increase of the solid loading content of slurry from 10% to 30%. Since the liquid camphene initially present in the slurry is converted into solid camphene that later sublimates to form the pore, the final porosity of porous ceramics is directly related to the volume of camphene in the slurry. Therefore, it is reasonable to suppose that the porosity of porous Y-SiAlON ceramics can be controlled by tuning the initial solid loading content.

The SEM micrographs of the sintered porous Y-SiAlON ceramics with different initial solid loading contents are shown in Fig. 2. It was observed that the porous structure was homogeneous throughout the entire samples. Lower solid loading content gave rise to a higher porosity and larger pore size, while the sintered Y-SiAlON walls became thinner.

It should be mentioned that the pore size measured by mercury porosimety (Table 1) is smaller than those estimated from the SEM micrographs shown in Fig. 2, wherein the pore size was 24 μm, 11 μm, and 7 μm at 10 vol%, 20 vol%, and 30 vol% respectively. The results imply that the pore channels were completely interconnected, consequently the relatively narrow pore represented the accurate pore size measured by mercury porosimetry [13].

3.3. Mechanical properties

Solid loading contents play a critical role in determining the porosities and porous structures of these sintered samples and consequently affect the compressive strength of samples. The flexural strength and fracture toughness of the obtained porous are listed in Table 1. When the porosity of sintered porous ceramic decreased from 62.3%

Table 1
Properties of the obtained porous α-SiAlON ceramics.

Solid content (vol%)	α/(α+β), (%)	Porosity (%)	Pore size ,μm	Flexural strength (MPa)	Fracture toughness (MPa m$^{1/2}$)	Dielectric loss at 15 GHz
10	79.4	64.3	19	72.4	1.20	1.4×10^{-2}
20	96.5	45.2	9	129.6	2.62	2.8×10^{-2}
30	100	23.1	6	190.2	3.48	2.0×10^{-2}

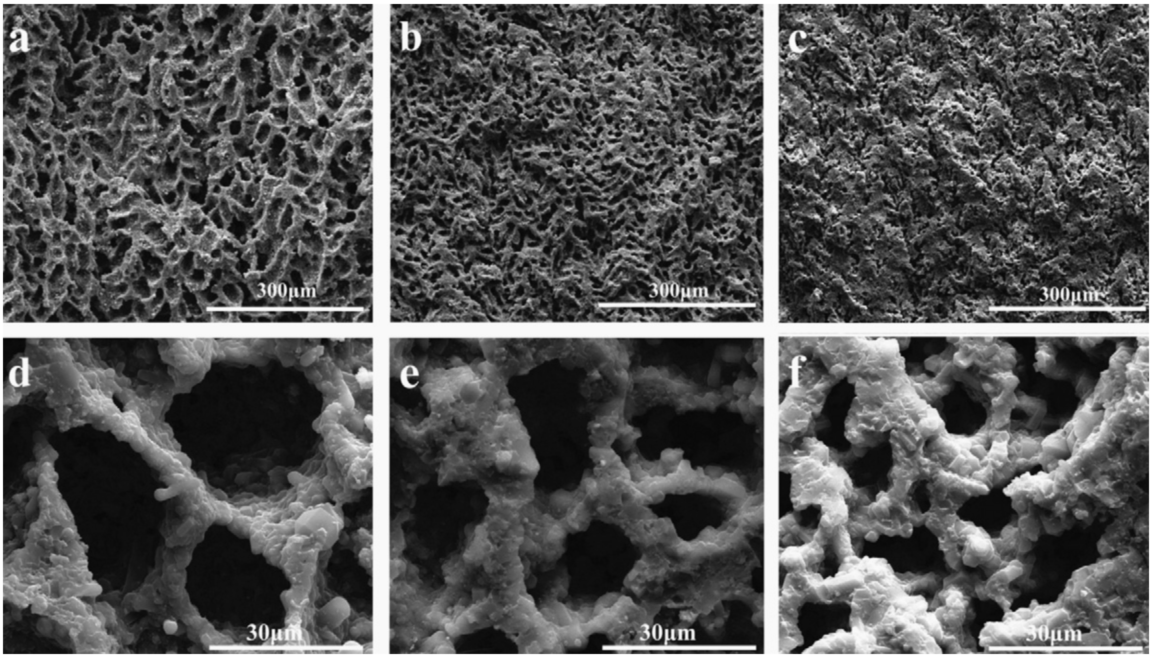

Fig. 2. SEM micrographs of the porous α-SiAlON ceramics sintered at 1900 °C for 1 h with different solid loading contents of (a), (d) 10 vol%; (b), (e) 20 vol%; and (c), (f) 30 vol%.

to 23.1%, the flexural strength increased from 72.4 Mpa to 190.2 Mpa with the fracture toughness increasing from 1.2 to 3.48 MPa m$^{1/2}$. These values are higher than the flexural strength of porous β-SiAlON with porosities 20–50% produced by partly sintering [14]. In general, the strength of porous ceramic is affected not only by the porosity but also by the formation of dense ceramic walls. From Fig. 2, we can see that the sintered Y-SiAlON ceramics walls showed full densification without any noticeable micropores and defects in the walls, regardless of initial solid loading. Therefore, the excellent mechanical properties were also attributed to the full dense Y-SiAlON ceramics walls.

3.4. Dielectric properties

Dielectric constant (ε') of α-SiAlON with different initial solid loading contents are measured in the frequency range 12.4–16 GHz and the corresponding profiles are presented in Fig. 3. All the materials exhibited reasonably stable dielectric constant values. The dielectric constant of these pore materials varied between 3.3 and 6.3, which is lower than that of the dense Y-α-SiAlON ceramic, 8.681.

For porous materials, if the pores are spheres, an approximation equation can be used to calculate the dielectric constant (ε') [15], as shown:

$$\varepsilon' = \varepsilon_m \left(1 - \frac{3P(\varepsilon_m - 1)}{2\varepsilon_m + 1 - P + P\varepsilon_m}\right) \tag{1}$$

where ε_m is dielectric constant of dense Y-α-SiAlON ceramic and P is porosity of porous ceramic.

When the porosity of porous α-SiAlON decreased from 62.3% to 23.1%, the measured dielectric constant of obtained porous α-SiAlON decreased from 6.3 to 3.3. While the calculated dielectric constant decreased from 6.39 to 3.31 according to Eq. (1), which is a good fit to the experimental data.

In general, the dielectric constant datas of porous ceramic were not only related to the porosity, but also to the change in phase assemblages. Y-α-SiAlON was formed completely in the porous α-SiAlON ceramic with initial solid loading constant 30 vol%; when the solid loading decreased to 10 vol%, the porous Y-α-SiAlON ceramic contained of 20.9% β-SiAlON, 79.1% Y-α-SiAlON and an intergranular glassy phase.

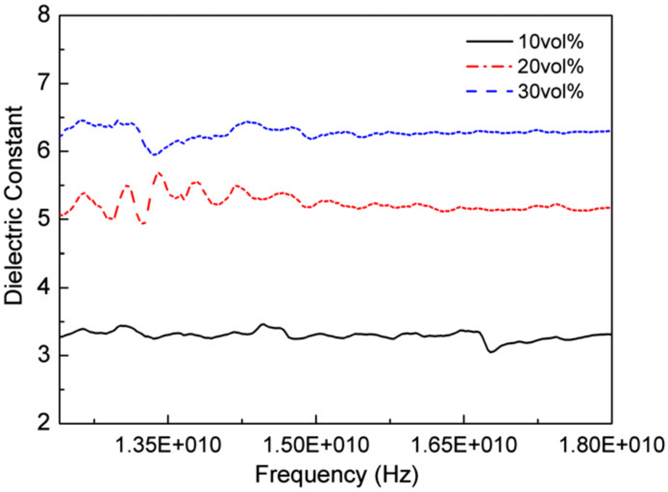

Fig. 3. Influence of initial solid loading content on dielectric constant of porous α-SiAlON ceramics sintered at 1900 °C for 1 h.

According to the mixture rule, the dielectric constant of the two-phase composite can be calculated by following Lichtencker's logarithmic equation:

$$Ln\,\varepsilon = V_1\,Ln\,\varepsilon_1 + V_2\,Ln\,\varepsilon_2 \tag{2}$$

where ε_1, ε_2 are the dielectric constant of phases 1 and 2, respectively, and V_1 and V_2 are the volume fraction of phases 1 and 2. The dielectric constant reported for β-SiAlON varied between 7.5 and 7.8 [16], which is lower than the dielectric constant of dense Y-α-SiAlON (8.681) [17]. The mixture rule would predict that the dielectric constant of dense α–β-SiAlON is smaller than that of dense Y-α-SiAlON. However, the variation of ε' between α-SiAlON and β-SiAlON was small, from which it can be deduced that ε' of porous SiAlON ceramics is unsusceptible to the phase assemblages. So it is reasonable to suppose that porosity is perhaps the dominating factor for the dielectric constant of porous α-SiAlON ceramic.

The dielectric loss (tan δ) of porousα-SiAlON ceramic with different initial solid loading contents at 15 GHz is listed in Table 1. The tan δ of these materials varied between 1.4×10^{-2} and 2.8×10^{-2}, which did not depend on the pore volume of the samples. It is unreasonable to consider that the loss may be related to the surface area of porosity for high porosity material, compared to the material with a small degree of porosity which has a very marked effect on loss [15].

4. Conclusion

We fabricated porous α-SiAlON ceramics with interconnected pore channels by using the camphene based freeze casting technique. The influence of initial solid loading content on the phase assemblages of porous SiAlON ceramics was investigated by XRD. α-SiAlON did not fully form in the sample with initial solid loading content of 10 vol%, due to the high porosity of 90 vol% and interconnected pore of the green body.

Initial solid loading played a primary role on the resulting porosity of the scaffolds. With the increase of initial solid loading content from 10 vol% to 30 vol%, the porosity decreased from 64.3% to 23.1% and the average pore size decreased from 19 μm to 8 μm. As a result, the flexural strength increased significantly from 72.4 MPa to 190.2 MPa; fracture toughness increased from 1.20 MPa m$^{1/2}$ to 3.48 MPa m$^{1/2}$; the dielectric constant increased from 3.3 to 6.3. The dielectric loss (tan δ) of obtained material varied between 1.4×10^{-2} and 2.8×10^{-2}, which did not depend on the porosity of samples.

In conclusion, this manufacturing technique shows a great potential for fabricated porous SiAlON ceramics with controlled porosity and appropriate mechanical and dielectric porosity for engineering application.

References

[1] A.R. Studart, U.T. Gonzenbach, E. Tervoort, L.J. Gauckler, Processing routes to macroporous ceramics: a review, Journal of the American Ceramic Society 89 (6) (2006) 1771–1789.

[2] S. Deville, Freeze-casting of porous ceramics: a review of current achievements and issues, Advanced Engineering Materials 10 (3) (2008) 155–169.

[3] S. Deville, E. Saiz, A.P. Tomsia, Ice-templated porous alumina structures, Acta Materialia 55 (6) (2007) 1965–1974.

[4] J. Han, C. Hong, X. Zhang, J. Du, W. Zhang, Highly porous ZrO_2 ceramics fabricated by a camphene-based freeze-casting route: microstructure and properties, Journal of the European Ceramic Society 30 (1) (2010) 53–60.

[5] T. Fukasawa, Z.Y. Deng, M. Ando, T. Ohji, S. Kanzaki, Synthesis of porous silicon nitride with unidirectionally aligned channels using freeze-drying process, Journal of the American Ceramic Society 85 (9) (2002) 2151–2155.

[6] B.H. Yoon, C.S. Park, H.E. Kim, Y.H. Koh, In situ synthesis of porous silicon carbide (SiC) ceramics decorated with SiC nanowires, Journal of the American Ceramic Society 90 (12) (2007) 3759–3766.

[7] Y. Shigegaki, M.E. Brito, K. Hirao, M. Toriyama, S. Kanzaki, Strain tolerant porous silicon nitride, Journal of the American Ceramic Society 80 (2) (1997) 495–498.

[8] F.L. Riley, Silicon nitride and related materials, Journal of the American Ceramic Society 83 (2) (2000) 245–265.

[9] I. Ganesh, S.M. Olhero, J.M.F. Ferreira, Phosphoric acid treated AlN powder for aqueous processing of net-shape dense AlN and beta-SiAlON parts, Advances in Applied Ceramics 108 (2) (2009) 111–117.

[10] K. Araki, J.W. Halloran, New freeze-casting technique for ceramics with sublimable vehicles, Journal of the American Ceramic Society 87 (10) (2004) 1859–1863.

[11] E.J. Lee, Y.H. Koh, B.H. Yoon, H.E. Kim, H.W. Kim, Highly porous hydroxyapatite bioceramics with interconnected pore channels using camphene-based freeze casting, Materials Letters 61 (112) (2007) 2270–2273.

[12] D. Salamon, Z. Shen, P. Sajgalik, Rapid formation of β-SiAlON during spark plasma sintering: its origin and implications, Journal of the European Ceramic Society 27 (6) (2007) 2541–2547.

[13] B.H. Yoon, Y.H. Koh, C.S. Park, H.E. Kim, Generation of large pore channels for bone tissue engineering using camphene-based freeze casting, Journal of the American Ceramic Society 90 (6) (2007) 1744–1752.

[14] J.F. Yang, Y. Beppu, G.J. Zhang, T. Ohji, S. Kanzaki, Synthesis and properties of porous single-phase beta -SiAlON ceramics, Journal of the American Ceramic Society 85 (7) (2002) 1879–1881.

[15] S.J. Penn, N.M. Alford, A. Templeton, X. Wang, M. Xu, M. Reece, K. Schrapel, Effect of porosity and grain size on the microwave dielectric properties of sintered alumina, Journal of the American Ceramic Society 80 (7) (1997) 1885–1888.

[16] Y.H. Seong, H.N. Kim, D.K. Kim, Dielectric properties of β-SiAlON at high temperature using perturbation method, Key Engineering Materials 403 (2009) 121–123.

[17] D.K. Kim, H.N. Kim, Y.H. Seong, S.S. Baek, Dielectric properties of SiAlON ceramics, Key Engineering Materials 403 (2009) 125–128.